RESEARCH FRONT

Full Paper

CSIRO PUBLISHING

Aust. J. Chem. **2009**, *62*, 334–340

www.publish.csiro.au/journals/ajc

Structural Characterization of Novel Ionic Salts Incorporating Trihalide Anions

Pamela M. Dean,[A,D] *Bronya R. Clare,*[A] *Vanessa Armel,*[B] *Jennifer M. Pringle,*[B,C] *Craig M. Forsyth,*[A] *Maria Forsyth,*[B,C] *and Douglas R. MacFarlane*[B]

[A]School of Chemistry, Monash University, Wellington Road, Clayton, VIC 3800, Australia.
[B]Department of Materials Engineering, Monash University, Wellington Road, Clayton, VIC 3800, Australia.
[C]Australian Research Council Centre of Excellence in Electromaterials Science, Monash University, Wellington Road, Clayton, VIC 3800, Australia.
[D]Corresponding author. Email: pamela.dean@sci.monash.edu.au

The crystal structures of several low-melting salts containing trihalide ions, namely 1-ethyl-3-methylimidazolium tribromide ([C_2mim][Br_3]), 1-ethyl-1-methylpyrrolidinium tribromide ([C_2mpyr][Br_3]), and 1-propyl-1-methylpyrrolidinium triiodide ([C_3mpyr][I_3]), are reported for the first time. Thermal analysis reveals that the tribromide salts are lower-melting than their monohalide analogues. Analysis of the crystal structures allows examination of the influence of the anions on the physical properties of the salts.

Manuscript received: 23 October 2008.
Final version: 17 February 2009.

Introduction

Ionic liquids (ILs) have potential application in a variety of contexts such as electrochemical devices, biocompatible solvents, sensor technologies, and pharmaceutical formulations.[1–4] Much research has been focussed on designing ILs via variation of the cation or anion, which each impart certain physicochemical properties, to achieve the desired physical properties for a specific application.[5–7] Recently, the trihalide-based ionic liquids have been pursued as reaction media for halogenations in organic synthesis.[8] Additionally, these hypervalent anions have been used in combination with 1,3-dialkylimidazolium, 1,2,3-trialkylimidazolium, and *N*-alkylpyridinium cations as electrolytes in dye-sensitized solar cells owing to the anions' electrochemical properties.[9] Recently, Bagno et al. have carried out a comparative study of a related set of 1-*n*-butyl-3-methylimidazolium ILs in order to understand the correlation between the physicochemical properties and structure of trihalide-based ILs, and thus ultimately design novel trihalide ILs for all the above-mentioned applications.[10] It was found that the trihalide-based ILs show a lower melting point and viscosity and a higher density compared with the rest of the imidazolium IL family.[10] Halide ILs are an interesting class of IL for applications such as lithium battery electrolytes[11] and cellulose dissolution[12] and as metal-free catalysts[13] but the use of these salts is hindered somewhat by their high melting points as well as general high hygroscopicity, viscosity, and tendency to decompose. In contrast, ILs utilizing trihalide anions have more desirable properties. Here, we report the first crystal structure analysis of low-melting salts utilizing trihalide anions in combination with typical IL organic cations, namely, 1-ethyl-3-methylimidazolium tribromide ([C_2mim][Br_3]), 1-ethyl-1-methylpyrrolidinium tribromide ([C_2mpyr][Br_3]), and 1-propyl-1-methylpyrrolidinium triiodide ([C_3mpyr][I_3]) and comparisons with the corresponding monohalide salts. The interactions between the anion and cation of the salt are of significant interest because distinctive properties ascribed to ILs are determined to a certain extent by these interactions.

Results

Thermal Analysis

Reproducible differential scanning calorimetry (DSC) analysis for [C_2mim][Br] and [C_2mim][Br_3] reveals a single broad endotherm corresponding to the melt. DSC analysis of [C_2mpyr][Br] and [C_3mpyr][I] reveals a single solid–solid phase transition and a sharp endotherm corresponding to the melt, as shown in Fig. 1 and Table 1. Interestingly, [C_2mpyr][Br_3] displays two solid–solid phase transitions, at $-25°C$ and $30°C$. The smaller endotherm seen at T_{onset} ~46°C corresponds to the melt; all traces are reversible (third run shown); the fact that the thermal events are reproducible suggests that they do not result from any permanent chemical change such as Br_2 evolution. Thermal analysis of the triiodide has not been carried out owing to the difficulty in purifying a sufficiently large sample for DSC analysis (see Experimental).

Other *N*-alkyl-1-methylpyrrolidinium salts have been found to have complex phase behaviour, where several solid–solid phase transitions occur before the melt. These solid–solid transitions occur owing to rotational and orientational motion of the ions within the crystal lattice.[14,15] Plastic crystalline materials often also display reduced entropy of fusion as a result.

10.1071/CH08456 0004-9425/09/040334

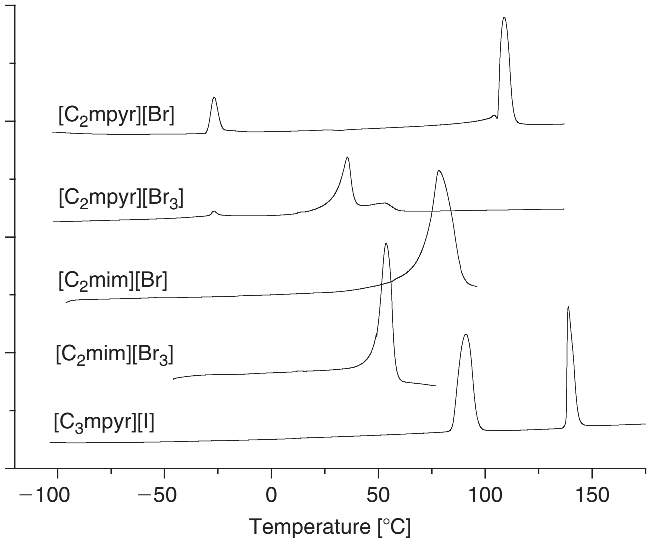

Fig. 1. DSC thermograms for [C$_2$mpyr][Br], [C$_2$mpyr][Br$_3$], [C$_2$mim][Br], [C$_2$mim][Br$_3$], and [C$_3$mpyr][I].

Table 1. Comparison of the thermal properties of the trihalide and monohalide salts

$T_{\text{s–s}}$, solid–solid transitions; T_{m}, entropy of fusion

Compound	$T_{\text{s–s}}$ [°C] ± 1°C$^{\text{A}}$	T_{m} [°C] ± 1°C
[C$_2$mpyr][Br]	−30	106
[C$_2$mpyr][Br$_3$]	−30 & 30	46
[C$_2$mim][Br]	–	71
[C$_2$mim][Br$_3$]	–	49
[C$_3$mpyr][I]	85	138
[C$_3$mpyr][I$_3$]	–	–

$^{\text{A}}$DSC measurements carried out from −150 to 150°C ([C$_2$mpyr][Br] and [C$_2$mpyr][Br$_3$]); −100 to 100°C ([C$_2$mim][Br]); −50 to 100°C ([C$_2$mim][Br$_3$]); and −150 to 200°C ([C$_3$mpyr][I]) at a scan rate of 10°C min^{-1}. Onset temperatures are reported in all cases.

In the case of molecular plastic crystals, the entropy of fusion is typically less than 20 J K^{-1} mol^{-1}.[16] In organic ionic plastic crystals, the entropy of fusion can be larger depending on the nature of the motions present in the plastic phase. The appearance of solid–solid phase transitions for [C$_2$mpyr][Br], [C$_2$mpyr][Br$_3$], and [C$_3$mpyr][I] and entropy of fusion values of 13.9, 5.0, and 12.8 J K^{-1} mol^{-1}, respectively, is quite consistent with plastic crystalline behaviour and, as such, these salts can also be expected to present a degree of crystalline disorder. In addition, the above thermal data reveal that the melting temperatures (T_{m}) of the tribromides are all significantly lower than their monohalide equivalent. In addition, despite the larger cation, the monoiodide salt displays a higher melting point than the bromide salts.

X-Ray Analysis

General Description of the Structures

Elaiwi et al.[17] have previously carried out the room-temperature crystallographic determination and analysis of [C$_2$mim][Br] (CCDC reference ZIBHUN). However, we have redetermined the structure at 123 K (private communication to the Cambridge Structural Database, deposition number CCDC 625783) and used these data for the current discussion. The salts [C$_2$mpyr][Br], [C$_2$mpyr][Br$_3$], [C$_3$mpyr][I],[18] and [C$_3$mpyr][I$_3$] crystallize in orthorhombic lattices, each with four pairs of ions occupying the unit cell. [C$_2$mim][Br] and [C$_2$mim][Br$_3$] crystallize in monoclinic and triclinic lattices, respectively, with four [C$_2$mim][Br] and two [C$_2$mim][Br$_3$] pairs of ions within the unit cell. The crystal data for all the structures are outlined in Table 2. One discrete ion pair for each new structure is shown as a thermal ellipsoid plot, along with the atom labelling scheme, in the Accessory Publication. The relative molar volume for all of the trihalide salts is ~70–90 Å higher than that of the corresponding monohalide, which is attributed to the larger size of the trihalide anions. The calculated densities for the trihalides are also considerably higher than for the monohalide salts.

Table 2. Crystal and refinement data for the monohalide and trihalide salts

	[C$_2$mim][Br]	[C$_2$mim][Br$_3$]	[C$_2$mpyr][Br]	[C$_2$mpyr][Br$_3$]	[C$_3$mpyr][I][18]	[C$_3$mpyr][I$_3$]
CCDC ref. code	625783	678422	678424	678423	WAWHIM	678425
Molecular formula	$C_6H_{11}N_2Br$	$C_6H_{11}N_2Br_3$	$C_7H_{16}N_1Br$	$C_7H_{16}N_1Br_3$	$C_8H_{18}N_1I$	$C_8H_{18}N_1I_3$
M [g mol^{-1}]	191.08	350.88	194.12	353.94	255.13	508.95
Crystal system	Monoclinic	Triclinic	Orthorhombic	Orthorhombic	Orthorhombic	Orthorhombic
Space group	$P2_1/c$	P-1	$P2_12_12_1$	$Pnma$	$P2_12_12_1$	$Pnma$
a [Å]	8.674(2)	6.8044(2)	7.2058(3)	15.011(2)	7.6816(8)	16.5206(12)
b [Å]	7.8814(2)	9.0431(3)	11.0507(4)	7.489(1)	11.8247(15)	8.0278(6)
c [Å]	12.4358(3)	9.1904(3)	11.1649(4)	10.332(2)	12.0196(14)	10.7594(8)
α [°]	90	104.24(2)	90	90	90	90
β [°]	109.26(10)	94.63(2)	90	90	90	90
γ [°]	90	97.77(2)	90	90	90	90
Z	4	2	4	4	4	4
V [Å^3]	802.57(52)	539.28(6)	889.05(6)	1161.5(3)	1091.8(2)	1426.96(18)
D_{calc} [g cm^{-3}]	1.581	2.161	1.450	2.024	1.552	2.369
Relative M_{v} [Å]	~200	~270	~220	~290	~270	~360
T [K]	123(2)	123(2)	123(2)	123(2)	170(2)	123(2)
R^{A}, wR_2^{B}	0.021, 0.0051	0.0292, 0.0741	0.0271, 0.0598	0.0396, 0.0900	–	0.0246, 0.0473
GOF$^{\text{C}}$	1.070	1.004	1.048	1.106		1.025

$^{\text{A}}R_1 = [\sum||F_{\text{o}}| - |F_{\text{c}}||]/\sum|F_{\text{o}}|$; $^{\text{B}}wR_2 = \{[\sum w(F_{\text{o}}^2 - F_{\text{c}}^2)^2]/[\sum w(F_{\text{o}}^2)^2]\}^{1/2}$; $^{\text{C}}S = [\sum[w(F_{\text{o}}^2 - F_{\text{c}}^2)^2]/(n-p)]^{1/2}$, where n is the number of data and p is the number of parameters refined (see Experimental).

Comparison of Cation and Anion Geometry

The [C$_2$mim] Cation

The dimensions of both of the carbon–nitrogen imidazolium skeletons do not vary significantly from each other and from that already reported.[17] The imidazolium rings are planar with N(1)–C(1) and N(2)–C(1) being shorter than N(1)–C(3) and N(2)–C(2), indicative of the aromatic nature of the ring. The β-carbon of the ethyl substituent lies out of the plane of the imidazolium ring, with a (C)–C(4)–C(5) angle of 112.09° for [C$_2$mim][Br$_3$] and 110.01° for [C$_2$mim][Br] (where (C) is the centroid of the plane).

The [C$_2$mpyr] Cation

The pyrrolidinium cations in [C$_2$mpyr][Br] and [C$_2$mpyr][Br$_3$] were modelled as disordered, with two separate positions located for all the carbon atoms (the nitrogen atom was common to both disordered components). In this disordered model, the pyrrolidinium ring of [C$_2$mpyr][Br] adopts two conformations, either twisted (component A) or half-chair (component B) as shown in Fig. 2 below. For [C$_2$mpyr][Br$_3$], the two cation components are related by a crystallographic mirror plane and adopt the half-chair conformation. The bond distances and angles of the C$_2$mpyr cations are all similar, except for minor variations, e.g. one disordered component of [C$_2$mpyr][Br] has a short C1A–C2A bond distance of 1.293(18) Å. The latter is most likely an artefact of the unrestrained refinement of the disordered cation and not geometrically significant. Henderson et al. have observed similar cation disorder in the phase III structure of [C$_2$mpyr][NTf$_2$]. This material exhibits a complex phase behaviour in which structural disorder appears to correlate with a plastic crystal phase.[19] Notably, both [C$_2$mpyr][Br] and [C$_2$mpyr][Br$_3$] exhibit solid–solid transitions below the melting temperature.

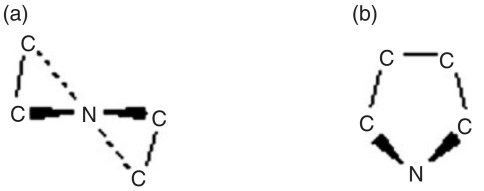

Fig. 2. Conformations displayed by the [C$_n$mpyr] rings, (a) twisted; and (b) half-chair.

The [C$_3$mpyr] Cation

As with the C$_2$mpyr cations above, the pyrrolidinium cations in [C$_3$mpyr][I] and [C$_3$mpyr][I$_3$] also displayed disorder in which either twisted or half-chair conformations were observed and some unusual bond distances were evident (e.g. in [C$_3$mpyr][I$_3$], C(4)–C(3) 1.664(8) Å and C(3)–C(2) 1.667(10) Å), presumably owing to the disorder. In both of the salts, the propyl chains adopt an energetically preferred *trans* zigzag conformation, with an N–C–C–C torsional angle of −172.9(3)° or −180.0(1)° for [C$_3$mpyr][I] and [C$_3$mpyr][I$_3$], respectively.

The [Br$_3$] and [I$_3$] Anions

All the trihalide anions adopt a linear geometry with Br(2)–Br(1)–Br(3) angles of 178.7(2)° or 179.17(4)° and an I(1)–I(2)–I(3) angle of 177.75(2)°, respectively. The two bond distances within each anion are dissimilar, in particular in the pyrrolidinium salts with ~0.13 Å and 0.12 Å difference in the X–X distances for the Br$_3^-$ and I$_3^-$, respectively (e.g. [C$_2$mim][Br$_3$]: Br(2)–Br(1), 2.555(1) Å; Br(1)–Br(3), 2.519(1) Å; [C$_2$mpyr][Br$_3$]: Br(2)–Br(1), 2.617(2) Å; Br(1)–Br(3), 2.483(2) Å; [C$_3$mpyr][I$_3$]: I(2)–I(1), 2.866(1) Å; I(3)–I(2), 2.991(1) Å).

Crystal Packing

All the extended structures show distinct layers of alternating anions and cations. As shown in Fig. 3, for the [C$_2$mim][Br] and [C$_2$mim][Br$_3$], the imidazolium cations show differing packing, with a parallel array of the [C$_2$mim] ring planes within the trihalide structure contrasting with the alternately canted packing in the monohalide.

Discussion

It is interesting to note that significant anion–anion interactions occur within the trihalide structures. The monohalides are generally further separated from the next nearest anion than those of the trihalides. For example; the shortest Br$^-\cdots$Br$^-$ distance in [C$_2$mpyr][Br] is 6.289 Å, whereas the corresponding

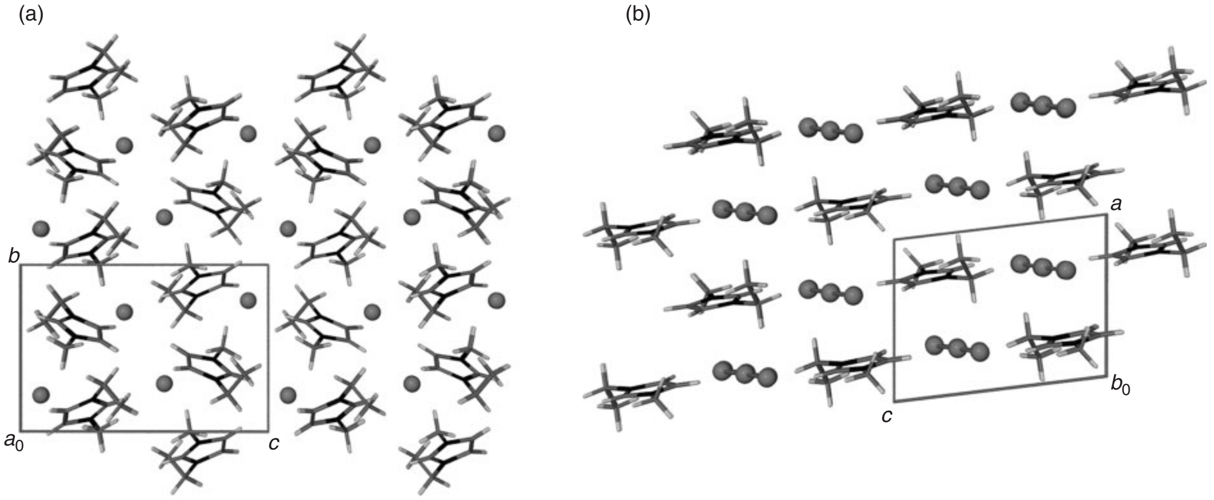

Fig. 3. The extended packing diagram of (a) [C$_2$mim][Br] and (b) [C$_2$mim][Br$_3$] as viewed down the *a*- and *b*-axis respectively, showing the layering motif.

$Br_3^-\cdots Br_3^-$ separation is 3.660 Å. Similarly, for [C$_3$mpyr][I] and [C$_3$mpyr][I$_3$], the $I^-\cdots I^-$ and $I_3^-\cdots I_3^-$ values are 6.588 Å and 3.993 Å, respectively. The distances are not so dramatic within the [C$_2$mim] salts, where the $Br^-\cdots Br^-$ distance of [C$_2$mim][Br] is 4.872 Å and the $Br_3^-\cdots Br_3^-$ distance in [C$_2$mim][Br$_3$] is 3.968 Å. These trihalide contacts generally fall within the sum of the van der Waals (vdW) radii of the atoms ($\sum$vdW Br 3.70 Å; I 3.96 Å),[20] suggesting a significant interaction. Additionally, the trihalide anions are lined up in a 'head-to-tail' zigzag motif as shown in Fig. 4. Consulting the literature, it is found that the same anionic alignment is seen within several triiodide complexes. These anions are reported to pack in tilted chains, linked via intermolecular contacts.[21–23] In addition, the trihalide bonds of the currently studied salts are much longer than the typical covalent bond lengths (Br–Br: ~2.28 Å; I–I: ~2.67 Å). This is indicative of hypervalent bonding, which is considerably weaker than covalent. The asymmetric X–X bonding suggests favourable formation of the bihalide anion via dissociation and consequently that the trihalide compounds may be good halide conductors via a Grotthus mechanism.

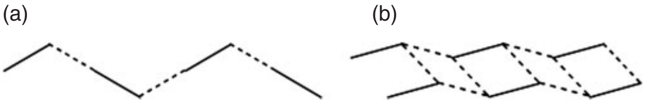

Fig. 4. Zig-zag alignment of the trihalides in (a) [C$_2$mim][Br$_3$]; and (b) [C$_2$mpyr][Br$_3$] and [C$_3$mpyr][I$_3$].

Table 3. Comparison of the shortest cation–anion N···X interaction distances of the mono- and trihalide salts

Symmetry operations: (i) $1-x, -y, 1-z$; (ii) $1+x, y, z$; (iii) $x-1/2, 1/2-y, 1/2-z$; (iv) $1/2+x, 1/2-y, -z$; (v) $x, y, z-1$

	Distance [Å]		Distance [Å]
[C$_2$mim][Br]	3.650	[C$_2$mim][Br$_3$]	3.787^{i}
[C$_2$mpyr][Br]	4.234^{ii}	[C$_2$mpyr][Br$_3$]	4.246^{iii}
[C$_3$mpyr][I]	4.733^{iv}	[C$_3$mpyr][I$_3$]	4.674^{v}

The degree of interaction between the anion and cation of each salt also influences the melting point, with a shorter anion (A^-)···cation (C^+) contact, indicative of stronger electrostatic interaction, contributing to a higher melting point. Table 3 displays the shortest cation–anion separations, as represented by the nominal centres of positive (N atom) and negative (central X atom) charge. The tribromide salts display greater N···X distances than the monobromides, which is consistent with the lower melting points and is likely to be a result of the more diffuse charge on the tribromide anion. In contrast, the triiodide salts display slightly shorter anion–cation interactions, suggesting that other factors are more dominant in determining the melting point.

In addition, an increase in the number of close contacts between the ions would theoretically increase the melting point. For the purpose of assessing these interactions, the distances are limited to those within the sum of the vdW radii (e.g. Br 2.87–3.07 Å; I 3.04–3.24 Å).[20] As described by Elaiwi et al.,[17] the ions in [C$_2$mim][Br] are interconnected by a 3D network of weak C–H···Br contacts, which are outlined in Table 4. In contrast, the corresponding tribromide salt [C$_2$mim][Br$_3$] has a predominantly 2D array of interactions (Fig. 5), with generally longer C–H···Br distances. For example, the shortest C–H···Br interaction in the monobromide salt is to the most acidic proton at C(1) (2.74 Å), whereas in the tribromide, the analogous interaction is now bifurcated (to Br(1) and Br(2)) with distances 2.92 Å and 2.95 Å, respectively. For the pyrrolidinium salts, the analysis of C–H···X interactions is complicated by the disorder of the cations in these structures. However, the general trend for longer C–H···X (X = Br, I) interactions for the trihalide salts than for the corresponding monohalide salts is also apparent (Table 4), although in all cases, these form a 3D network of interactions. Consequently, it would appear that the strength of the short-range interactions is a contributing factor to the lower melting points of the trihalide salts.

Table 4. C–H···X distances [Å] found in the mono- and trihalide salts

	X$_{donor}$–H	Br	Br$_3$	I	I$_3$
[C$_2$mim]	C(1)	2.74	2.92	–	–
	C(2)		2.95		
	C(3)	2.84	2.95	–	–
	C(4)	2.97/2.97	–	–	–
	C(5)	–	2.95	–	–
	C(6)	2.88	–	–	–
[C$_2$mpyr]	C(2)	–	3.06	–	–
	C(4)	2.87/3.08 (2.92/2.96)^A	2.99	–	–
	C(5)	3.05/3.09	2.91/3.01	–	–
	C(6)	2.76/2.95 (2.76/2.87)	2.93/2.97	–	–
[C$_3$mpyr]	C(3)	–	–	–	3.08/3.09
	C(4)	–	–	3.19	–
	C(5)	–	–	3.17	3.26
	C(6)	–	–	3.16/3.17	3.28

^{A}The values in parentheses correspond to the second component of the disordered cation. The standardized numbering scheme used for compiling Table 4 is as follows:

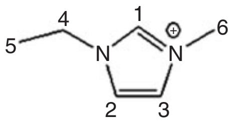

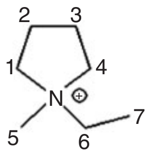

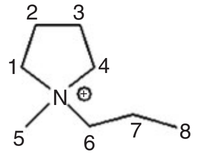

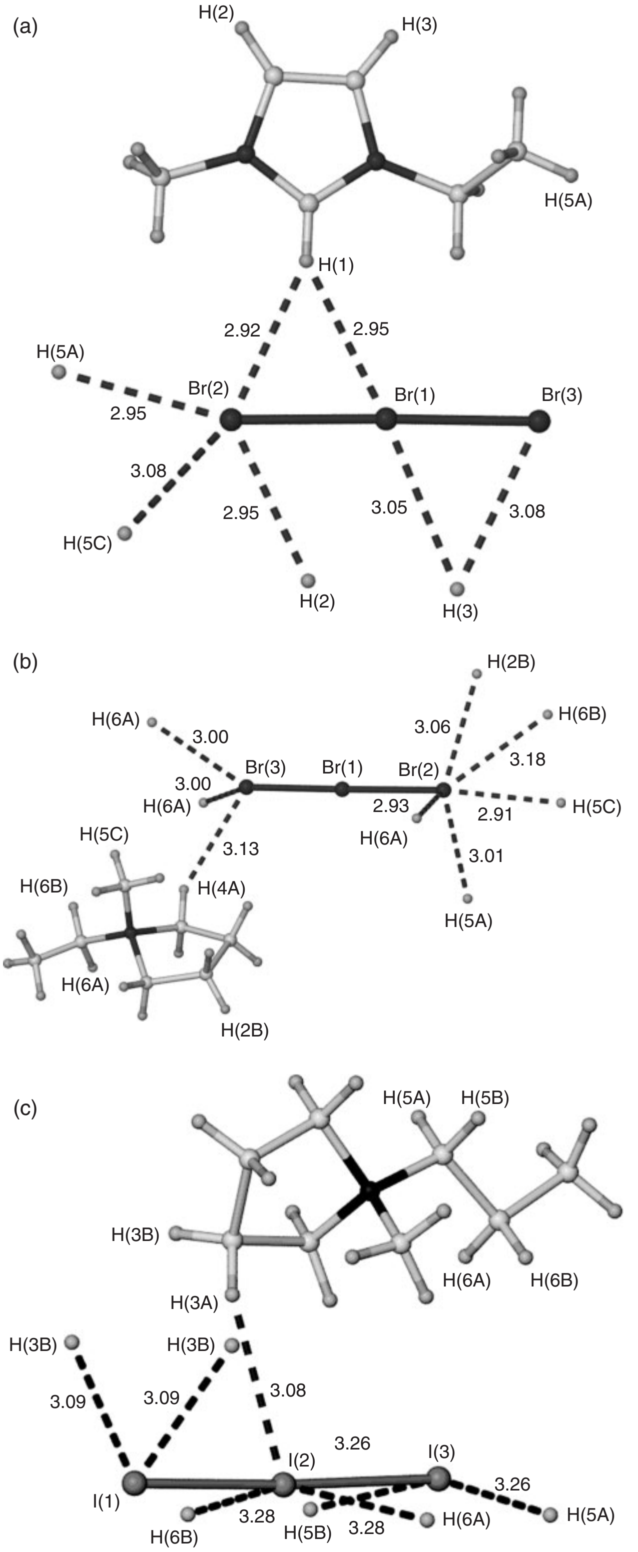

Fig. 5. C–H···X interactions in [C_2mim][Br_3], [C_2mpyr][Br_3], and [C_3mpyr][I_3] salts. The interactions shown represent those from one component of the disordered cations only. H···X distances are indicated in Å.

The directional nature of X^-···H–donor contacts and the hydrogen bonding acceptor ability of halogens has been reported.[24] This acceptor functionality is evidenced in the occurrence of several hydrogen close contacts for the studied compounds; for example, [C_2mpyr][Br_3] displays several close contacts at Br(3) and Br(2) (Fig. 5). The bifurcated bonding pattern within [C_2mim][Br_3] and [C_3mpyr][I_3] has also been reported in other halogen-containing compounds.[25]

Conclusion

Analysis of the low-melting salts 1-ethyl-3-methylimidazolium tribromide ([C_2mim][Br_3]) and 1-ethyl-3-methylpyrrolidinium tribromide ([C_2mpyr][Br_3]) show that these salts display lower melting points than those of the monohalide equivalents. X-ray crystal structure analysis of the new salts, including 1-propyl-1-methylpyrrolidinium triiodide ([C_3mpyr][I_3]), confirmed the existence of anion–cation close contacts. Analysis of much weaker C–H···X contacts revealed generally longer distances for the trihalide salts, which may contribute to their lower melting points relative to the corresponding monohalide salts. Furthermore, the trihalide salts exhibited chains of closely spaced anions (within the sum of the vdW distance) along with asymmetric X–X bond lengths, which suggest that these materials may be able to transfer halide anions through dissociation to the X_2 and X^- and thus are good candidates for halide ion conductivity.

Experimental

Salt Preparation and Preliminary Characterization

General

NMR spectra were recorded on a Bruker DPX-200 spectrometer at 200 MHz using deuterated dimethylsulfoxide or deuterium oxide as the solvent; all samples were referenced to the residual solvent resonances at 2.50 and 4.79 ppm, respectively. ESI were carried out on a Micromass Platform II API QMS electrospray mass spectrometer with a cone voltage of 25 or 35 V. Methanol was used as the mobile phase unless specified otherwise. Analyses were conducted in both positive (ESI^+) and negative (ESI^-) modes. DSC experiments were performed on a TA Instruments Perkin–Elmer Q100. Samples of mass 5–20 mg were sealed in a vented aluminium pan and placed in the furnace with a 50 mL min^{-1} nitrogen stream; the temperature was raised at 10°C min^{-1}.

1-Ethyl-1-methylpyrrolidinium Bromide ([C_2mpyr][Br])

Bromoethane (40.0 mL, 0.536 mol) in 150 mL isopropanol was added dropwise to methylpyrrolidine (50.0 mL, 0.481 mol) in 150 mL isopropanol and the resulting solution was stirred under a nitrogen atmosphere for 24 h. The volume was reduced to ~200 mL under vacuum, ~200 mL *n*-hexanes was added and the solution was left at −10°C to crystallize. The solid product was filtered, washed thoroughly with *n*-hexanes, and dried under vacuum. Yield 60.5 g, 64.8%. δ_H (D_2O) 3.54 (m, 4H), 3.46 (q, *J* 7.3, 2H), 3.07 (s, 3H), 2.26 (m, 4H), 1.43 (t, *J* 7.3, 3H). *m/z* (ESI^+) 113.9 ($C_7H_{16}N^+$); *m/z* (ESI^-) 78.7 (Br^-).

1-Ethyl-3-methylimidazolium Bromide ([C_2mim][Br])

Bromoethane (50.0 mL, 0.670 mol) in 150 mL isopropanol was added dropwise to 1-methylimidazole (48.0 mL, 0.602 mol) in 50 mL isopropanol and the resulting solution was stirred under a nitrogen atmosphere for 24 h. Volatiles were removed under vacuum and the solid yellow product was dissolved in 100 mL acetonitrile and stirred over activated carbon (SAJ first grade, Aldrich) for 24 h. Carbon was removed by filtration and the solid product was crystallized and recrystallized from acetonitrile at −10°C. Yield 62.1 g, 54.0%. δ_H (D_2O) 7.55 (s, 1H), 7.48 (s, 1H), 4.27 (q, *J* 7.3, 2H), 3.96 (s, 3H), 1.56 (t, *J* 7.3, 3H). *m/z* (ESI$^+$) 110.9 ([C$_2$mim]$^+$); *m/z* (ESI$^-$) 80.8 (Br^{-1}).

1-Propyl-1-methylpyrrolidinium Iodide ([C$_3$mpyr][I])

1-Methylpyrrolidine (18.0 mL, 0.176 mol) was dissolved in 100 mL of ethyl acetate. Iodopropane (20.0 mL, 0.205 mol) was added dropwise. The mixture was stirred under a nitrogen atmosphere, overnight, at room temperature. The solid product was filtered and washed with ethyl acetate. The product was dried under vacuum for 2 days. Yield 27.4 g, 65.0%. δ_H (D$_2$O) 3.57 (m, 4H), 3.34 (m, 2H), 3.07 (s, 3H), 2.25 (m, 4H), 1.92–1.76 (m, 2H), 1.02 (t, *J* 7.3, 3H). *m/z* (ESI$^+$) 127.9 ($C_8H_{18}N^+$); *m/z* (ESI$^-$) 126.7 (I$^-$).

1-Ethyl-1-methylpyrrolidinium Tribromide ([C$_2$mpyr][Br$_3$])

Elemental bromine (0.5 mL, 9.76 mmol) was added dropwise to [C$_2$mpyr][Br] (1.24 g, 6.39 mmol). The reaction mixture was stirred at 60°C for 2 h. Excess elemental bromine was removed under vacuum and the final product was crystallized at −10°C from acetonitrile. δ_H ([D$_6$]DMSO) 1.27 (t, *J* 7.3, 3H), 2.05–2.18 (m, 4H), 2.96 (s, 3H), 3.37 (q, *J* 7.3, 2H), 3.47–3.35 (m, 4H).

1-Ethyl-3-methylimidazolium Tribromide ([C$_2$mim][Br$_3$])

This compound was synthesized in an analogous way to [C$_2$mpyr][Br$_3$], using the same relative quantities. δ_H ([D$_6$]DMSO) 1.42 (t, *J* 7.3, 3H), 3.85 (s, 3H), 4.19 (q, *J* 7.3, 2H), 7.77 (s, 1H), 7.69 (s, 1H), 9.12 (s, 1H).

1-Propyl-1-methylpyrrolidinium Triiodide ([C$_3$mpyr][I$_3$])

X-ray-quality crystals of [C$_3$mpyr][I$_3$] were obtained overnight from an electrolyte mixture containing lithium iodide (0.0269 g, 0.201 mmol), iodine (0.0788 g, 0.310 mmol), 4-*tert*-butylpyridine (0.0781 g, 0.577 mmol), and 1-propyl-1-methylpyrrolidinium iodide (0.123 g, 0.482 mmol), which was made up to 1.00 mL with 1-propyl-1-methylpyrrolidinium bis(trifluoromethanesulfonyl)amide.

Structure Determination and Crystal Data

General

Intensity data were collected on a Bruker X8 APEX KAPPA CCD single crystal X-ray diffractometer (thin slice ϕ and ω scans, $2\theta_{max} = 57°$, graphite-monochromated Mo-Kα X-rays, $\lambda = 0.71073$ Å, $T = 123$ K). All crystals were coated in Paratone oil (Exxon Chemical Co., TX, USA) immediately after isolation and cooled in a stream of nitrogen vapour (15 cm^3 min^{-1}, Oxford Cryostream cooler) on the diffractometer. Mounting of the trihalide crystals was particularly challenging owing to the highly deliquescent nature of the salts. Handling of the monohalide salts was less challenging, suggesting a lower hydrophilicity. Structures were solved and refined with the *SHELX-97* software in conjunction with the *X-Seed* Graphical User Interface.[26] An empirical absorption correction was applied using *SADABS*.[26] Crystal data are listed in Table 2 above.

1-Ethyl-3-methylimidazolium Tribromide ([C$_2$mim][Br$_3$])

The structure was solved by direct methods and refined by full matrix least-squares with anisotropic thermal parameters for all non-hydrogen atoms. The hydrogen atom positions were located in the difference Fourier map but were placed in calculated positions with isotropic temperature factors assigned at $U_{iso}(H) = xU_{eq}(C)$, where $x = 1.5$ for methyl and 1.2 for all other C atoms. Final refinement based on 2695 reflection data converged to R_1 [1969 data with $I > 2\sigma(I)$] = 0.0292, $wR_2 = 0.0741$ (all data), and goodness-of-fit on $F^2 = 1.004$. Weighting scheme: $w = 1/[\sigma^2(F_o^2) + (0.0353P)^2]$ where $P = 1/3(F_o^2 + 2F_c^2)$.

1-Ethyl-1-methylpyrrolidinium Bromide ([C$_2$mpyr][Br])

The structure was solved using direct methods and expanded by subsequent least-squares refinement and difference Fourier cycles. Carbon atoms C(1), C(2), C(3), C(4), C(6), and C(7) were modelled as disordered with two alternative positions for each atom. The site-occupancy factors (s.o.f.s) were fixed at 0.5 after trial refinement. All non-hydrogen atoms were assigned anisotropic temperature factors; all the hydrogen atoms were placed in idealized positions in a riding model with $U_{iso}(H) = xU_{eq}(C)$, where $x = 1.5$ for methyl and 1.2 for all other C atoms. Full-matrix least-squares refinement, based on 2397 reflection data, converged to R_1 [1840 data with $I > 2\sigma(I)$] = 0.0271, $wR_2 = 0.0598$ (all data), and goodness-of-fit on $F^2 = 1.048$. Weighting scheme: $w = 1/[\sigma^2(F_o^2) + (0.0194P)^2 + 0.4900P]$ where $P = 1/3(F_o^2 + 2F_c^2)$.

1-Ethyl-1-methylpyrrolidinium Tribromide ([C$_2$mpyr][Br$_3$])

The structure was solved using direct methods and expanded by subsequent least-squares refinement and difference Fourier cycles. The atoms Br(1), Br(2), Br(3), C(1), C(2), C(7), and N(1) were situated on a crystallographic mirror plane and the remaining carbon atoms C(3), C(4), C(5), and C(6) were disordered over two positions (symmetry: *x*, *y*, *z* and *x*, 1/2 − *y*, *z*). S.o.f.s were fixed at 0.5. All non-hydrogen atoms were refined with anisotropic thermal parameters; all the hydrogen atoms were placed in idealized positions using a riding model (C–H distances in the range 0.95–1.00 Å and $U_{iso}(H) = xU_{eq}(C)$), where $x = 1.5$ for methyl and 1.2 for all other C atoms. Full-matrix least-squares refinement, based on 1439 reflection data, converged to R_1 [1090 data with $I > 2\sigma(I)$] = 0.0396, $wR_2 = 0.0900$ (all data), and goodness-of-fit on $F^2 = 1.106$. Weighting scheme: $w = 1/[\sigma^2(F_o^2) + (0.0303P)^2 + 3.2706P]$ where $P = 1/3(F_o^2 + 2F_c^2)$. Attempted refinement in a monoclinic system was less satisfactory.

1-Propyl-1-methylpyrrolidinium Triiodide ([C$_3$mpyr][I$_3$])

The structure was solved using direct methods expanded by subsequent least-squares refinement and difference Fourier cycles. The atoms I(1), I(2), I(3), N(1), C(1), C(2), C(5), C(6), and C(7) were situated on a crystallographic mirror plane and the remaining carbon atoms, C(3) and C(4), were disordered over two positions (symmetry: *x*, *y*, *z* and *x*, 1/2 − *y*, *z*) and refined with a fixed s.o.f. at 0.5. The atoms C(4) and C(4′) were restrained to occupy the same coordinates and have the same atomic displacement parameter and correspond to either one of the α ring carbon atoms or the methyl group carbon atom in each disorder component. Additionally, the C(3)–C(4) bond distance was restrained to a reasonable value. All non-hydrogen atoms were refined with anisotropic thermal parameters and all the hydrogen atoms were placed in idealized positions in a riding model (C–H distances in the range 0.95–1.00 Å and $U_{iso}(H) = 1.2U_{eq}(C)$). The highest remaining electron density peak (1.02 e Å^{-3}) is located at a distance of ~0.7 Å from I(1). Full-matrix least-squares refinement, based on 1907 reflection data, converged to R_1 [1534 data with $I > 2\sigma(I)$] = 0.0246, $wR_2 = 0.0473$

(all data), and goodness-of-fit on $F^2 = 1.025$. Weighting scheme: $w = 1/[\sigma^2(F_\mathrm{o}^2) + (0.0112P)^2 + 3.4145P]$ where $P = 1/3(F_\mathrm{o}^2 + 2F_\mathrm{c}^2)$.

Accessory Publication

Detailed crystallographic diagrams of a discrete ion pair for [C$_2$mim][Br], [C$_2$mpyr][Br], [C$_3$mpyr][I], [C$_2$mim][Br$_3$], [C$_2$mpyr][Br$_3$], and [C$_3$mpyr][I$_3$] and the full crystallographic information files are available from the Journal's website.

Acknowledgements

P.M.D. is grateful to Monash University for the Monash Graduate Scholarship and Monash International Postgraduate Research Scholarship, J.M.P. and D.R.M. are grateful to the Australian Research Council for a QEII Fellowship and Federation Fellowship respectively.

References

[1] D. R. MacFarlane, M. Forsyth, P. Howlett, J. Pringle, J. Sun, G. Annat, W. Neil, E. Izgorodina, *Acc. Chem. Res.* **2007**, *40*, 1165. doi:10.1021/AR7000952

[2] K. Fujita, D. R. MacFarlane, M. Forsyth, M. Yoshizawa-Fujita, K. Murata, N. Nakamura, H. Ohno, *Biomacromolecules* **2007**, *8*, 2080. doi:10.1021/BM070041O

[3] J. H. Poplin, R. P. Swatloski, J. D. Holbrey, S. K. Spear, A. Metlen, M. Gratzel, M. K. Nazeeruddin, R. D. Rogers, *Chem. Commun.* **2007**, 2025. doi:10.1039/B704651K

[4] W. L. Hough, M. Smiglak, H. Rodriguez, R. P. Swatloski, S. K. Spear, D. T. Daly, J. Pernak, J. E. Grisel, R. D. Carliss, M. D. Soutullo, J. H. Davis, Jr, R. D. Rogers, *N. J. Chem.* **2007**, *31*, 1429. doi:10.1039/B706677P

[5] T. Itoh, K. Kude, S. Hayase, M. Kawatsura, *Tetrahedron Lett.* **2007**, *48*, 7774. doi:10.1016/J.TETLET.2007.09.010

[6] H. Ohno, *Bull. Chem. Soc. Jpn.* **2006**, *79*, 1665. doi:10.1246/BCSJ.79.1665

[7] J. G. Huddleston, A. E. Visser, W. M. Reichert, H. D. Willauer, G. A. Broker, R. D. Rogers, *Green Chem.* **2001**, *3*, 156. doi:10.1039/B103275P

[8] O. Bortolini, M. Bottai, C. Chiappe, V. Conte, D. Pieraccini, *Green Chem.* **2002**, *4*, 621. doi:10.1039/B209436N

[9] M. Gorlov, H. Pettersson, A. Hagfeldt, L. Kloo, *Inorg. Chem.* **2007**, *46*, 3566. doi:10.1021/IC062244B

[10] A. Bagno, C. Butts, C. Chiappe, F. D'Amico, J. C. D. Lord, D. Pieraccini, F. Rastrelli, *Org. Biomol. Chem.* **2005**, *3*, 1624. doi:10.1039/B502654G

[11] J. Shin, W. A. Henderson, S. Passerini, *Electrochem. Solid-State Lett.* **2005**, *8*, A125. doi:10.1149/1.1850387

[12] (a) R. P. Swatloski, S. K. Spear, J. D. Holbrey, R. D. Rogers, *J. Am. Chem. Soc.* **2002**, *124*, 4974. doi:10.1021/JA025790M
(b) S. Zhu, Y. Wu, Q. Chen, Z. Yu, C. Wang, S. Jin, Y. Ding, G. Wu, *Green Chem.* **2006**, *8*, 325. doi:10.1039/B601395C

[13] W. Wang, L. Wu, Y. Huang, B. Li, *Polym. Int.* **2008**, *57*, 872. doi:10.1002/PI.2421

[14] W. A. Henderson, V. G. Young, Jr, W. Pearson, S. Passerini, H. C. De Long, P. C. Trulove, *J. Phys. Condens. Matter* **2006**, *18*, 10377. doi:10.1088/0953-8984/18/46/006

[15] D. R. Macfarlane, P. Meakin, N. Amini, M. Forsyth, *J. Phys. Condens. Matter* **2001**, *13*, 8257. doi:10.1088/0953-8984/13/36/303

[16] J. Timmermans, *J. Phys. Chem. Solids* **1961**, *18*, 1. doi:10.1016/0022-3697(61)90076-2

[17] A. Elaiwi, P. B. Hitchcock, K. R. Seddon, N. Srinivasan, Y. Tan, T. Welton, J. A. Zora, *J. Chem. Soc., Dalton Trans.* **1995**, 3467. doi:10.1039/DT9950003467

[18] A. Babai, A. Mudring, *Acta Crystallographica* **2005**, *E61*, o2913. doi:10.1107/S1600536805025481

[19] W. A. Henderson, V. G. Young, Jr, S. Passerini, P. C. Trulove, H. C. De Long, *Chem. Mater.* **2006**, *18*, 934. doi:10.1021/CM051936F

[20] A. Bondi, *J. Phys. Chem.* **1964**, *68*, 441. doi:10.1021/J100785A001

[21] E. R. Gordon, R. B. Walsh, W. T. Pennington, T. W. Hanks, *J. Chem. Crystallogr.* **2003**, *33*, 385. doi:10.1023/A:1024278013820

[22] E. Miyazaki, Y. Morita, Y. Yakiyama, S. Maki, Y. Umemoto, M. Ohmoto, K. Nakasuji, *Chem. Lett.* **2007**, *36*, 1102. doi:10.1246/CL.2007.1102

[23] O. N. Kazheva, G. G. Aleksandrov, O. A. D'yachenko, M. S. Chernov'yants, E. O. Lykova, I. E. Tolpygin, I. M. Raskita, *Russ. J. Coord. Chem.* **2004**, *30*, 636.

[24] L. Brammer, E. A. Bruton, P. Sherwood, *Cryst. Growth Des.* **2001**, *1*, 277. doi:10.1021/CG015522K

[25] J. C. Mareque Rivas, L. Brammer, *Inorg. Chem.* **1998**, *37*, 4756. doi:10.1021/IC9805269

[26] (a) G. M. Sheldrick, *Acta Crystallogr. Sect. A Fundamental Crystallography* **2008**, *A64*, 112.
(b) L. J. Barbour, *J. Supramol. Chem.* **2001**, *1*, 189. doi:10.1016/S1472-7862(02)00030-8
(c) G. M. Sheldrick, *SADABS Program for Scaling and Absorption Correction of Area Detector Data* **1997** (University of Göttingen: Göttingen).